High spatial resolution analysis of the distribution of sulfate reduction and sulfide oxidation in hypoxic sediment in a eutrophic estuary

Rathnayake M. L. D. Rathnayake, Shogo Sugahara, Hideaki Maki, Gen Kanaya, Yasushi Seike and Hisashi Satoh

ABSTRACT

Bottom hypoxia and consequential hydrogen sulfide (H_2S) release from sediment in eutrophic estuaries is a major global environmental issue. We investigated dissolved oxygen, pH and H_2S concentration profiles with microsensors and by sectioning sediment cores followed by colorimetric analysis. The results of these analyses were then compared with the physicochemical properties of the bottom water and sediment samples to determine their relationships with H_2S production in sediment. High organic matter and fine particle composition of the sediment reduced the oxidation-reduction potential, stimulating H_2S production. Use of a microsensor enabled measurement of H_2S concentration profiles with submillimetre resolution, whereas the conventional sediment-sectioning method gave H_2S measurements with a spatial resolution of 10 mm. Furthermore, microsensor measurements revealed H_2S consumption occurring at the sediment surface in both the microbial mat and the sediment anoxic layer, which were not observed with sectioning. This H_2S consumption prevented H_2S release into the overlying water. However, the microsensor measurements had the potential to underestimate H_2S concentrations. We propose that a combination of several techniques to measure microbial activity and determine its relationships with physicochemical properties of the sediment is essential to understanding the sulfur cycle under hypoxic conditions in eutrophic sediments.

Key words | concentration profiles, microsensors, particle composition, physicochemical properties, sediment core sectioning, white filamentous bacteria

Rathnayake M. L. D. Rathnayake
Department of Civil Engineering, Faculty of Engineering,
University of Peradeniya,
20400,
Sri Lanka

Shogo Sugahara
Yasushi Seike
Interdisciplinary Faculty of Science and Engineering,
Shimane University,
Matsue,
Shimane 690-8504,
Japan

Hideaki Maki
Gen Kanaya
National Institute for Environmental Studies (NIES),
16-2, Onogawa,
Tsukuba,
Ibaraki 305-8506,
Japan

Hisashi Satoh (corresponding author)
Division of Environmental Engineering, Faculty of Engineering,
Hokkaido University,
North-13, West-8,
Sapporo 060-8628,
Japan
E-mail: *qsatoh@eng.hokudai.ac.jp*

INTRODUCTION

Eutrophication caused by anthropogenic activity is a major environmental problem in estuaries. In particular, urbanized and industrialized watersheds can result in large inputs of organic matter and nutrients into estuaries. Degradation of organic matter in an estuary results in reduction or complete depletion of dissolved oxygen (DO) in the bottom water, which are termed hypoxia and anoxia, respectively (Kodama *et al.* 2010; Sato *et al.* 2012). Low DO can lead to increased mortality of macrobenthic fauna and fish, as well as to accelerated production of hydrogen sulfide (H_2S) in hypoxic bottom sediments (Valdemarsen *et al.* 2009). Because H_2S is both toxic to benthic biota and consumes DO, H_2S production is harmful to estuarine ecosystems and should be prevented (Kodama *et al.* 2010). However, the mechanism of H_2S production is complicated and depends on sediment physicochemical properties including DO, oxidation-reduction potential (ORP), pH, and nitrate, sulfate and organic matter concentrations, as well as sediment grain size and porosity (Valdemarsen *et al.* 2009); therefore, it is difficult to control.

To understand the mechanism of H_2S production, H_2S concentration profiles in the sediment have been examined using several different techniques. Traditionally, H_2S profiles have been determined by sectioning sediment cores and performing colorimetric H_2S determination of interstitial water samples obtained by squeezing or *in situ* equilibration of dialysis cells (Koretsky *et al.* 2007). However, the difficulties associated with fine scale sediment

doi: 10.2166/wst.2016.516

sectioning result in a spatial resolution of only a few centimetres. At the sediment–water interface, steep concentration gradients can exist at a submillimetre scale, making the sectioning technique inadequate (Nakamura *et al.* 2004). Therefore, other analytical methods with higher spatial resolution (e.g., diffusive equilibration (DET) and diffusive gradients in thin-films (DGT), planar optodes and microsensors) have been developed and used for the measurement of H_2S concentration profiles. DET and DGT techniques are used to investigate the two-dimensional distribution of H_2S in the sediment. In these methods, H_2S diffusing into thin hydrogel is trapped by an immobilized binding agent, then subjected to colorimetric determination (Pages *et al.* 2014). These techniques typically have a spatial resolution in the millimetre scale (Gregusova & Docekal 2013); however, they require labor-intensive and time-consuming steps such as gel preparation and several days of gel deployment for equilibration and H_2S determination. Planar optodes allow two-dimensional measurements of dissolved matter at higher spatial (micrometre) and temporal (minutes) resolution than either the DET or DGT technique. Planar optodes have been used to determine the two-dimensional distribution and dynamics of DO and pH (Larsen *et al.* 2011) and CO_2 (Zhu & Aller 2010) in both sediment and soil. However, the types of fluorescent indicators available for planar optodes are limited; therefore, they can only be used for a few analytes (Glud 2008).

Microsensors, which have been developed for a variety of analytes in the last three decades, may provide a solution to the shortfalls of the previous methods. Microsensors are biochemical sensors with a tip having a diameter at the micrometre scale. Because of their small size, microsensors have been used to determine the concentration profiles of dissolved matter with minimal disturbance of the sediment sample. Revsbech *et al.* (1980), who were the first to use an oxygen (O_2) microsensor for sediment analysis, revealed the steep concentration gradients of DO and heterogeneity of its distribution. Since then, various types of microelectrodes have been developed and introduced to determine concentration profiles of H_2S (Kühl *et al.* 1998), N_2O (Binnerup *et al.* 1992) and metals (Luther *et al.* 1998) in lake, estuary and continental shelf sediments. However, no studies have investigated the relationship between the measured H_2S concentration profile and the physicochemical properties of hypoxic and/or anoxic sediment in eutrophic estuaries. An understanding of the relationship between H_2S production/consumption and the physicochemical properties of the water–sediment interface is essential for the prevention of H_2S release and subsequent hypoxia in the sediment. In this study, DO, pH and H_2S concentration profiles at the water–sediment interface of hypoxic sediment were monitored by microsensors. H_2S concentration profiles in the sediment samples were determined using the H_2S microsensor and by sectioning sediment cores and then subjecting the sections to colorimetric analysis. The sediment samples were obtained from Tokyo Bay because previous studies have demonstrated that eutrophication causes hypoxia from spring to autumn in this system (Sato *et al.* 2012). H_2S profiles were compared with physicochemical properties of the sediment samples to better understand the role of sediment physicochemistry in the sulfur cycle.

MATERIALS AND METHODS

Samples

Samples of overlying water and sediments were collected from three sites in Tokyo Bay between May 2010 and August 2011: the Chiba Light Beacon vicinity (34°34′05″N, 140°2′45″E, 12–13 m water depth), Sanmaizu (35°36′53″N, 139°51′34″E, 6–7 m water depth) and the Tokyo Light Beacon (35°34′9″N, 139°50′51″E, 15–16 m water depth), hereafter referred to as Sites 1, 2 and 3, respectively (Figure 1). Vertical profiles of the physicochemical parameters (DO, temperature and salinity) in the bottom water were obtained *in situ* using a sounder (Hydrolab DataSonde 4a; Hach Environmental, Loveland, CO, USA). ORP was measured with a glass electrode (9300-10D, Horiba, Kyoto, Japan).

Sediment cores were sampled *in situ* using acrylic tubes (4 cm inner diameter, 40 cm in length) inserted directly into the sediment by divers. After plugging both ends of the acrylic tubes with rubber lids, the tubes were transported onto boats and stored in cooling boxes until laboratory analysis. Sediment grain size and composition were determined using the sieving and precipitation method following the test method for particle size distribution of soil (Japanese Industrial Standards A 1204:2009 and Japanese Geotechnical Society (JGS) 0131-2009) described in the *Laboratory Testing Standards of Geomaterials* published by the JGS. Sediments were dried to constant weight at 105 °C (approximately 2 h) to determine water content (%). Subsamples (approximately 1 g) were burned for 2 h at 650 °C to determine loss on ignition (LOI). Acid volatile sulfide (AVS) content in the sediment samples was assayed using HYDROTEC-S (GASTEC, Japan). Briefly, approximately

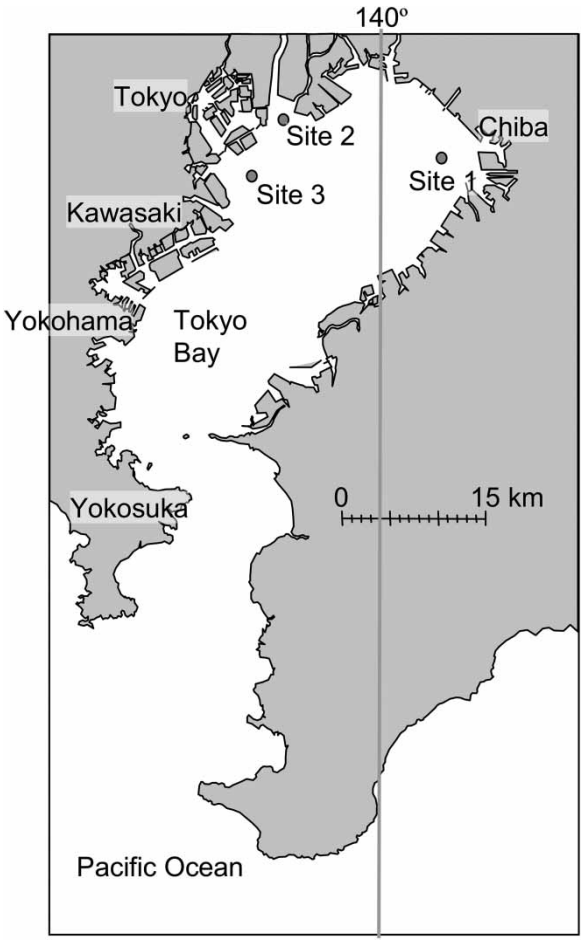

Figure 1 | Map of Tokyo Bay and the location of the study sites.

1 g of wet sediment was transferred into a glass vessel, which acted as a H_2S gas generation tube, to which 2 mL of 18 N sulfuric acid was added. The H_2S gas generated was then drawn into a H_2S detecting tube by suction via a sealed glass cap and a gas sampling pump. The ORP and temperature were measured directly by inserting a glass electrode into the sediment samples.

Colorimetric determination of H_2S in interstitial water of the sediment samples

Colorimetric determination of dissolved sulfide, which was defined as the sum of H_2S, HS^- and S^{2-}, was accomplished according to the modified methods of Cline (1969) and Sugahara *et al.* (2010). The sulfide concentration measured using this method was referred to as $\Sigma(H_2S)$. Each sediment core was horizontally sliced 1, 2 and 3 cm from the top of the core by stepwise extrusion from the corer using a plunger. Each sediment slice was then placed in a plastic cup, and a sample was immediately taken using a 30 mL glass syringe. The samples were volumetrically adjusted to 2.5 mL, after which 20 mL of N_2-gas-purged, DO-free deionized water was added directly to each syringe via a three-way stopcock. The sediment samples were suspended in the deionized water by manual shaking after ejecting the air from the syringes. Each suspended sediment sample was then filtered with a cellulose acetate membrane filter cartridge (25 mm diameter, 0.45 μm pore size, DISMIC-25CS, Advantec, Japan), and 10 mL of filtrate was introduced into a new syringe via a three-way stopcock. One millilitre of 0.23 M zinc acetate solution was then added directly to the filtrate in each syringe to form zinc sulfide, after which 2 mL of 6 N hydrochloric acid solution was added to the zinc sulfide, and the $\Sigma(H_2S)$ concentration was determined using methylene blue. This process involves the addition of 0.5 mL of coloring reagent (a mixture of *N*,*N*-dimethyl *p*-phenylene diamine sulfate (DMPDS) and ferric chloride ($FeCl_3$)) to the acidified samples, which are then rested for 15 minutes to allow the formation of methylene blue as a chromophore. The methylene blue concentration was then determined by spectrophotometry at a wavelength of 667 nm, 2 hours after the addition of DMPDS solution. Two types of coloring reagent solutions were used according to the $\Sigma(H_2S)$ concentration: (1) 0.4 g of DMPDS and 0.6 g of $FeCl_3 \cdot 6H_2O$ containing 100 mL of 6 N HCl for low $\Sigma(H_2S)$ concentration samples (<2 mg $\Sigma(H_2S)$ L^{-1}) and (2) 4.0 g of DMPDS and 6.0 g of $FeCl_3 \cdot 6H_2O$ containing 100 mL of 6 N HCl for high $\Sigma(H_2S)$ concentration samples (<30 mg $\Sigma(H_2S)$ L^{-1}). Determination of high $\Sigma(H_2S)$ concentration samples required dilution of the methylene blue solution with deionized water to adjust the concentration to within the quantitative range of absorbance values measurable by the spectrophotometer.

Microsensor measurements

Steady-state concentration profiles of DO, T-H_2S ($\Sigma(H_2S)$ measured with a H_2S microsensor) and pH were measured according to the method described by Okabe *et al.* (1999). Clark-type O_2 and H_2S microsensors and a pH microsensor were purchased from Unisense (Aarhus, Denmark) and calibrated according to the manufacturer instructions. DO, T-H_2S and pH concentration profiles in the sediment samples were obtained using a micromanipulator at intervals of 200 to 500 μm. The microsensor tip was positioned with a dissecting microscope (model Stemi 2000; Carl Zeiss). Three concentration profiles for each species were measured at different points in each sediment sample.

The net volumetric T-H_2S production rate (R(T-H_2S)) in each sediment sample was calculated from the mean steady-state concentration profiles of T-H_2S using Fick's second law of diffusion as described by Okabe *et al.* (1999):

$$\frac{dC(x,t)}{dt} = D_s \frac{d^2C(x,t)}{dx^2} + R(x)$$

where C is the concentration of the chemical species at depth x and time t, D_s is the sediment diffusion coefficient of the chemical species, and R is the production rate of the chemical species at depth x. Positive and negative values of R(T-H_2S) indicate T-H_2S production (i.e., sulfate reduction) and consumption, respectively. We used the D_s values previously determined in sediments: $D_s(O_2) = 1.31 \times 10^{-5}$ cm^{-2} s^{-1} (Nakamura *et al.* 2004) and Ds (H_2S) $= 1.39 \times 10^{-5}$ cm^{-2} s^{-1} (Okabe *et al.* 1999). The rates were calculated as described previously by Okabe *et al.* (1999). The local diffusive fluxes of T-H_2S (J(T-H_2S)) and DO ($J(O_2)$) were calculated using Fick's first law of diffusion (Okabe *et al.* 1999):

$$J(x) = -\Phi D_s \frac{dC(x)}{dx}$$

where Φ is the sediment porosity measured in this study.

To examine the effectiveness of each method of sulfide measurement, the ratio of sulfide determined by the microsensor (quantity of T-H_2S) to that determined by colorimetric determination (quantity of $\Sigma(H_2S)$) was calculated. The quantity of T-H_2S was estimated by integrating the T-H_2S concentration profile over a depth of 10 mm, while that of $\Sigma(H_2S)$ was estimated as $\Sigma(H_2S)$ multiplied by 10 mm of depth.

RESULTS

Physicochemical properties of the sediment and bottom water

The average percentage of sand, silt and clay in the sediment samples taken from three sites in the inner Tokyo Bay between May 2010 and August 2011 ($n = 9$) are shown in Table 1. The samples were taken at a sediment depth of 0.1 m. In Sites 1 and 3, the sediment was mainly composed of silt and clay, whereas sand comprised 52% of the sediment in Site 2.

The physicochemical properties of the bottom water and of the sediment samples at a sediment depth of 3 cm for each of the three study sites are shown in Table 2. Sediment AVS concentrations were higher and ORP values were lower at Site 3 than at Sites 1 or 2. LOI, which is an indicator of organic matter content, was higher at Site 3 than at the other sites. Sediment water content was high at Sites 1 and 3, but low at Site 2, indicating more extensive dewatering and compaction of the sediment at Site 2. DO in the bottom water was below 15 μM (0.5 mg L^{-1}) at all sites on all three sampling dates, except for Site 2 in July 2010 (37 μM), when ORP in the bottom water was also much higher (+165 mV) than at other sites or other times. Overall, sediment AVS concentrations were relatively high at Site 3, which was characterized by fine sediments, lower ORP and higher LOI.

Table 1 | Average (maximum–minimum) percentage of sand, silt and clay by dry weight in sediment samples taken from three sites in Tokyo Bay between May 2010 and August 2011 ($n = 9$)

	Site 1	Site 2	Site 3
Sediment (particle size)			
Medium sand (0.425–0.850 mm)	3 (13–0)	6 (16–1)	0 (0–0)
Fine sand (0.106–0.425 mm)	5 (17–2)	46 (74–10)	1 (2–0)
Silt	71 (88–46)	32 (63–4)	82 (90–72)
Clay	20 (28–10)	15 (28–6)	17 (27–9)

Vertical distribution of H_2S concentrations and rates of sulfate reduction and sulfide oxidation at the sediment surface

The vertical distribution of bulk $\Sigma(H_2S)$ at the sediment surface of each site was determined by the colorimetric method (Figure 2). Bulk $\Sigma(H_2S)$ concentrations increased with depth in all samples. Bulk $\Sigma(H_2S)$ concentrations in the deepest layer (i.e., 20–30 mm depth) of the sediment were highest at Site 3 (2,000–12,000 μM) and lowest at Site 2 (<250 μM). AVS concentrations followed a similar trend among sites (Table 2).

The steady-state concentration profiles of DO, T-H_2S and pH measured with microsensors are depicted in Figure 2. DO was depleted at the sediment surface in most samples; thus, DO profiles are only shown for Sites 1 and 2 in July 2010 (Figure 2(a) and (b)). DO penetrated only 0.4 mm into the sediment at Site 2 in July 2010 (Figure 2(a)), even when the DO of the bottom water was 100 μM. DO depletion was likely caused by a combination of high microbial respiration during oxidation of organic matter,

Table 2 | Physical and chemical properties of the surface sediment and bottom water at three sites in Tokyo Bay

	Site 1			Site 2			Site 3		
	2010 July	2010 August	2011 August	2010 July	2010 August	2011 August	2010 July	2010 August	2011 August
Sediment (0–3 cm)									
AVS (mg g-dry^{-1})	0.8	1	1.3	1.8	1.2	1.1	3.3	2.3	2.6
LOI (%)	12	12	13	8	10	7	15	15	16
ORP (mV)	–329	–399	–387	–311	–299	–309	–411	–410	–388
Water content (%)	80	79	82	62	70	59	90	90	90
Temperature (°C)	26	24	24	26	28	25	22	19	23
Bottom water									
DO (μM)	2	3	9	37	9	6	14	7	7
ORP (mV)	–124	–92	N.M.	165	–18	N.M.	–125	–38	N.M.
Temperature (°C)	24	23	23	25	28	24	22	21	21
Salinity	27	32	34	26	27	33	29	33	35

N.M.: not measured; AVS: acid volatile sulfide; LOI: loss on ignition; ORP: oxidation-reduction potential; DO: dissolved oxygen.

low DO in the bottom water, low liquid flow rate at the sediment surface during measurement, and/or fine silt or clay particles inhibiting DO diffusion into the sediment. $J(O_2)$ fluxes, which were calculated from the linear DO concentration profiles at the sediment surface, were 0.049 and 0.045 μmol cm^{-2} h^{-1} at Sites 1 and 2, respectively, in July 2010. Because the samples were incubated in the dark, DO showed no net increase, indicating insignificant photosynthesis in all samples. These reducing conditions resulted in sulfate reduction in the sediment. The T-H_2S concentrations increased with depth at all three sites, although they were higher at Sites 1 and 3 (~2,700 μM) than at Site 2 (<600 μM) on each sampling date. The T-H_2S concentrations were highest in August 2010 for all samples.

The standard deviation of the T-H_2S concentration at each sediment depth was lower than 5%, except for Site 2 in August 2010 (<20%) and August 2011 (<60%). These findings indicate that the vertical distribution of sulfate reduction and sulfide oxidation was relatively homogeneous. Therefore, the values of R(T-H_2S) were calculated from the average steady-state concentration profiles of T-H_2S by diffusion reaction modeling (Figure 3). In addition, J(T-H_2S) values were calculated from the linear T-H_2S concentration profiles of the measured sediment depth range (Table 3). R(T-H_2S) in Sites 1 and 3 in August 2010 were relatively high (<0.26 μmol cm^{-3} h^{-1}), resulting in high J(T-H_2S) in these samples (Table 3). Thus, significant concentrations of H_2S were detected in the bottom waters at Site 1 (0.02 mg S L^{-1}) and Site 3 (0.74 mg S L^{-1}). In some sediment samples, rates of T-H_2S oxidation were so low that T-H_2S reached the sediment surface (Table 3) and diffused into the overlying water (Figure 2). In contrast, at Sites 1 and 3 in July 2010 and Site 2 in August 2010, T-H_2S was completely oxidized at the surface sediment (Table 3). H_2S oxidation at the surface sediment is vital for preventing toxic H_2S release from the sediment into the overlying water.

DISCUSSION

Among the study sites in Tokyo Bay, sulfate reduction, which was represented by AVS, bulk Σ(H_2S) and T-H_2S accumulation, was highest at Site 3 on each sampling date. Moreover, Site 3 was characterized by higher LOI (organic matter) than Sites 1 or 2 (Table 2). High organic matter in the sediment can stimulate sulfate reduction via consumption of DO followed by a decrease in ORP in sediment or by providing increased quantities of electron donors for sulfate-reducing bacteria (Holmer & Storkholm 2001). Rates of sulfate reduction (R(T-H_2S)) in this study (<0.26 μmol cm^{-3} h^{-1}) were substantially higher than those of natural sediments in acidic lakes (Kühl *et al.* 1998) and sandy intertidal sediments (de Beer *et al.* 2005) (<0.01 μmol cm^{-3} h^{-1}), while they were comparable to those of anaerobic sewer biofilm (Mohanakrishnan *et al.* 2009) and organic-rich sludge in a marine aquaculture system (Schwermer *et al.* 2010) (<1.0 μmol cm^{-3} h^{-1}). Thus, these results indicate a massive input of organic matter to Tokyo Bay sediments is occurring. Moreover, the fine

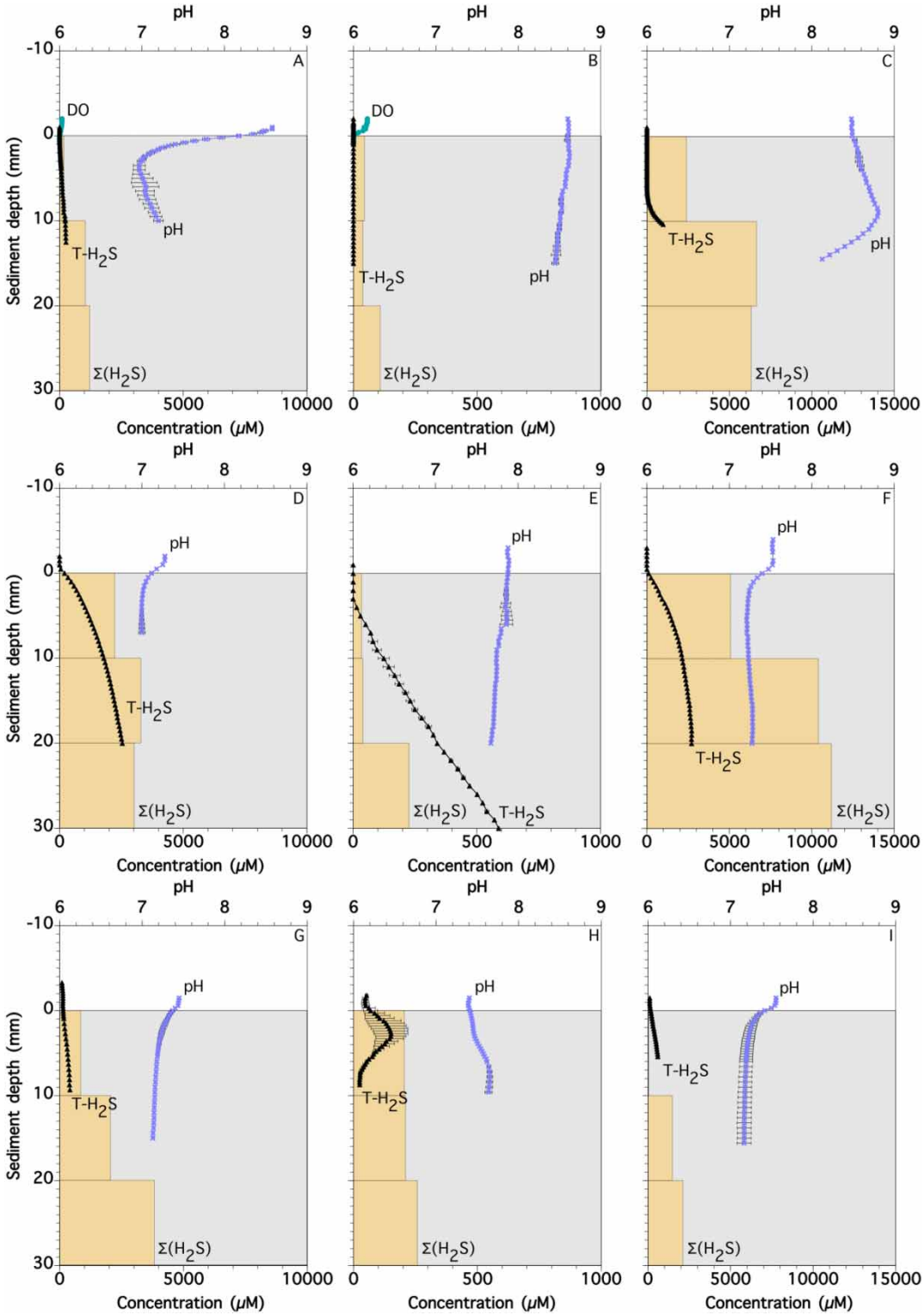

Figure 2 | Vertical distribution of bulk $\Sigma(H_2S)$ (boxes) and concentration profiles of DO (filled circle), T-H_2S (filled triangle) and pH (cross) in the surface sediment of three study sites: Site 1 (a), Site 2 (b) and Site 3 (c) in July 2010; Site 1 (d), Site 2 (e) and Site 3 (f) in August 2010; and Site 1 (g), Site 2 (h) and Site 3 (i) in August 2011. Note that the maximal value of the horizontal axis is different between the study sites. The concentration profiles of DO, T-H_2S and pH are average values ($n = 3$) and error bars represent the standard deviations of triplicate measurements. Zero on the vertical axis corresponds to the surface of the sediment.

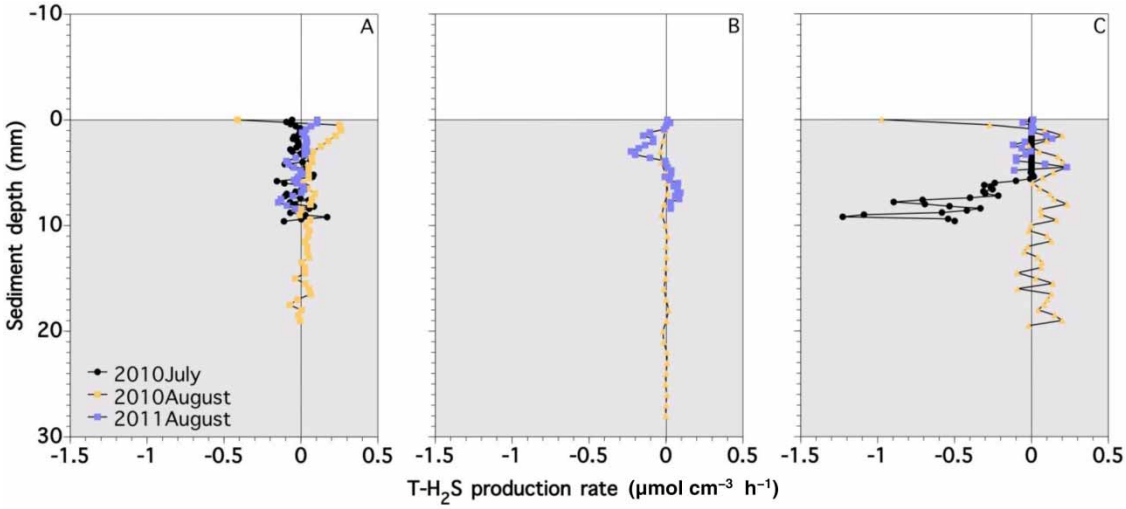

Figure 3 | Vertical distribution and magnitude of the net volumetric T-H_2S production rates (R(T-H_2S)) in the sediment samples at Site 1 (a), Site 2 (b) and Site 3 (c). The rates were calculated based on the corresponding concentration profiles shown in Figure 2. Negative values indicate consumption. Zero on the vertical axis corresponds to the surface of the sediment.

Table 3 | Local diffusive fluxes of T-H_2S (J(T-H_2S)), zone in which J(T-H_2S) was calculated, T-H_2S concentration at the sediment surface (Conc.) and ratio of the quantities of T-H_2S and $\Sigma(H_2S)$

	Site 1				Site 2				Site 3			
	J(T-H_2S) (μmol cm^{-2} h^{-1})	Zone (mm)	Conc. (μM)	Ratio	J(T-H_2S) (μmol cm^{-2} h^{-1})	Zone (mm)	Conc. (μM)	Ratio	J(T-H_2S) (μmol cm^{-2} h^{-1})	Zone (mm)	Conc. (μM)	Ratio
July 2010	0.011	0 – 9.8	0	0.5	0		0	0	0.246	9.4 – 10.4	0	0.01
August 2010	0.121	0 – 2.0	201	0.5	0.011	3.0 – 30	0	1.21	0.146	0 – 2.0	109	0.26
August 2011	0.018	0 – 3.9	142	0.29	0.021	0 – 1.5	69	0.42	0.041	0 – 5.1	170	9.7

particles constituting the sediment at Site 3 may reduce the diffusive transport of oxygenated species (e.g., DO, nitrate and ferric oxide) and eventually stimulate sulfate reduction. Kodama *et al.* (2010) also reported severe bottom hypoxia (<45 μM of DO) in a northern area of Tokyo Bay, including all sites in this study in August 2005, and found H_2S concentrations were higher in silt and clay sediments than in sand.

Comparison of the T-H_2S concentration profiles measured by a microsensor with the vertical distribution of bulk $\Sigma(H_2S)$ demonstrated that T-H_2S could be determined at depth intervals of 0.2 mm, whereas bulk $\Sigma(H_2S)$ concentration intervals were 10 mm. The microsensor measurements showed that T-H_2S concentrations were changing at the submillimetre scale. It should be noted that the T-H_2S was completely oxidized at a depth of 5.5 mm in the Site 3 sediment in July 2010, and that no T-H_2S was detected in the surface layer of the sediment, but a microbial mat of white filamentous bacteria, approximately 10 mm thick, was found on the sediment surface (Figure 4). This was likely to consist of *Beggiatoa* spp., which can oxidize H_2S with DO and/or nitrate (Kamp *et al.* 2006). It is well known that mats of *Beggiatoa* at the sediment surface can prevent the diffusion of toxic H_2S into overlying waters because biological H_2S oxidation is much more rapid and efficient than chemical H_2S oxidation (Kamp *et al.* 2006). DO was depleted at the sediment surface because of low DO in the bottom water layer, and the sum of nitrate and nitrite concentrations in the bottom water was only 6 μM at Site 3 in July 2010. In addition, electric currents may not have directly connected oxygen reduction at the sediment surface to sulfide oxidation at deeper sediment depths in this sample, as pH was observed to increase between the oxygen reduction and sulfide oxidation zones (Pfeffer *et al.* 2012). Therefore, an electron acceptor for *Beggiatoa*-like bacteria has not been identified. Furthermore, a

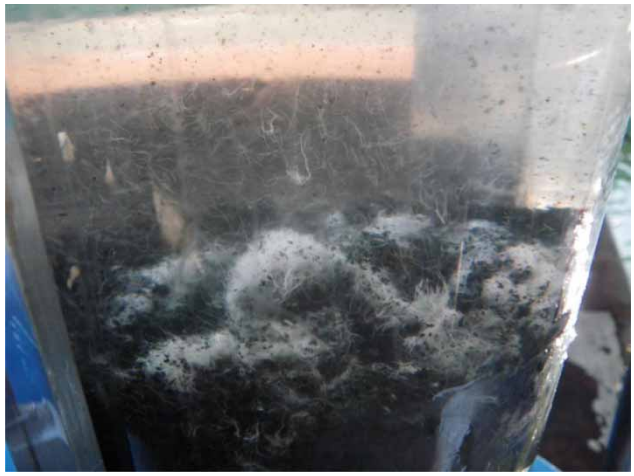

Figure 4 | Photograph of the surface sediment sampled in Site 3 in July 2010. Inner diameter of the acrylic tube is 4 cm.

decrease in T-H_2S concentrations was observed in anoxic sediments deeper than 3 mm at Site 2 in August 2011. Decreased T-H_2S may have been caused by bioturbation providing oxygen and/or nitrate (Rabouille *et al.* 2009) or by upward diffusion of dissolved Fe^{2+} reacting with H_2S to form FeS under reducing conditions in the sediment (Dittrich *et al.* 2009). Without the use of a microsensor, these unusual phenomena would have been overlooked.

T-H_2S and bulk $\Sigma(H_2S)$ concentration profiles showed some similarities; specifically, both increased with sediment depth and were lower in sediments at Site 2 than at Sites 1 or 3. However, the ratio of the quantity of T-H_2S to bulk $\Sigma(H_2S)$ in the top 10 mm of sediment ranged from 0.01 to 10 (Table 3), indicating that microsensor measurements may frequently underestimate H_2S concentrations. Although the exact reason remains unknown, one explanation may be that T-H_2S concentration profiles were measured in the laboratory under different conditions than those *in situ*. Alternatively, the T-H_2S concentration profiles may not necessarily represent an averaged concentration profile because of inadequate replication (only three points per sediment sample). Nevertheless, our results indicate that microsensor measurement is necessary to properly analyze the sulfur cycle in sediment at the submillimetre scale.

CONCLUSIONS

The H_2S concentration profiles and rates of sulfate reduction and sulfide oxidation in the sediment of Tokyo Bay were determined at a submillimetre scale using a microsensor, whereas the spatial resolution of the sediment core sectioning method was 10 mm. The calculated T-H_2S production rates in some eutrophic sediment samples were much higher than those found in natural sediments in other studies. Among the sediment properties measured, high organic matter content and fine particle composition (i.e., silt and clay) may primarily be responsible for the inhibition of DO diffusion into the sediment, the low ORP and the stimulation of sulfate reduction at the surface sediment in Tokyo Bay. Sulfate reduction and H_2S oxidation in the sediment showed dynamic variation with depth at the submillimetre scale and differed among sites. Without the use of a microsensor, these spatial dynamics with depth would have been overlooked. Overall, microsensor measurements provided critical insight into the sulfur cycle in the hypoxic surface sediment of a eutrophic estuary.

REFERENCES

Binnerup, S. J., Jensen, K., Revsbech, N. P., Jensen, M. H. & Sorensen, J. 1992 Denitrification, dissimilatory reduction of nitrate to ammonium, and nitrification in a bioturbated estuarine sediment as measured with 15N and microsensor techniques. *Applied and Environmental Microbiology* **58** (1), 303–313.

Cline, J. D. 1969 Spectrophotometric determination of hydrogen sulfide in natural waters. *Limnology and Oceanography* **14** (3), 454–458.

de Beer, D., Wenzhöfer, F., Ferdelman, T. G., Boehme, S. E., Huettel, M., van Beusekom, J. E. E., Böttcher, M. E., Musat, N. & Dubilier, N. 2005 Transport and mineralization rates in North Sea sandy intertidal sediments, Sylt-Rømø Basin, Waddensea. *Limnology and Oceanography* **50** (1), 113–127.

Dittrich, M., Wehrli, B. & Reichert, P. 2009 Lake sediments during the transient eutrophication period: reactive-transport model and identifiability study. *Ecological Modelling* **220** (20), 2751–2769.

Glud, R. N. 2008 Oxygen dynamics of marine sediments. *Marine Biology Research* **4** (4), 243–289.

Gregusova, M. & Docekal, B. 2013 High resolution characterization of uranium in sediments by DGT and DET techniques ACA-S-12-2197. *Analytica Chimica Acta* **763**, 50–56.

Holmer, M. & Storkholm, P. 2001 Sulphate reduction and sulphur cycling in lake sediments: a review. *Freshwater Biology* **46** (4), 431–451.

Kamp, A., Stief, P. & Schulz-Vogt, H. N. 2006 Anaerobic sulfide oxidation with nitrate by a freshwater *Beggiatoa* enrichment culture. *Applied and Environmental Microbiology* **72** (7), 4755–4760.

Kodama, K., Oyama, M., Kume, G., Serizawa, S., Shiraishi, H., Shibata, Y., Shimizu, M. & Horiguchi, T. 2010 Impaired megabenthic community structure caused by summer hypoxia in a eutrophic coastal bay. *Ecotoxicology* **19** (3), 479–492.

Koretsky, C. M., Haveman, M., Beuving, L., Cuellar, A., Shattuck, T. & Wagner, M. 2007 Spatial variation of redox and trace

metal geochemistry in a minerotrophic fen. *Biogeochemistry* **86** (1), 33–62.

Kühl, M., Steuckart, C., Eickert, G. & Jeroschewski, P. 1998 A H_2S microsensor for profiling biofilms and sediments: application in an acidic lake sediment. *Aquatic Microbial Ecology* **15** (2), 201–209.

Larsen, M., Borisov, S. M., Grunwald, B., Klimant, I. & Glud, R. N. 2011 A simple and inexpensive high resolution color ratiometric planar optode imaging approach: application to oxygen and pH sensing. *Limnology and Oceanography: Methods* **9**, 348–360.

Luther, G. W., Brendel, P. J., Lewis, B. L., Sundby, B., Lefrançois, L., Silverberg, N. & Nuzzio, D. B. 1998 Simultaneous measurement of O_2, Mn, Fe, I^-, and S(-II) in marine pore waters with a solid-state voltammetric microelectrode. *Limnology and Oceanography* **43** (2), 325–333.

Mohanakrishnan, J., Gutierrez, O., Sharma, K. R., Guisasola, A., Werner, U., Meyer, R. L., Keller, J. & Yuan, Z. 2009 Impact of nitrate addition on biofilm properties and activities in rising main sewers. *Water Research* **43** (17), 4225–4237.

Nakamura, Y., Satoh, H., Okabe, S. & Watanabe, Y. 2004 Photosynthesis in sediments determined at high spatial resolution by the use of microelectrodes. *Water Research* **38** (9), 2439–2447.

Okabe, S., Itoh, T., Satoh, H. & Watanabe, Y. 1999 Analyses of spatial distributions of sulfate-reducing bacteria and their activity in aerobic wastewater biofilms. *Applied and Environmental Microbiology* **65** (11), 5107–5116.

Pages, A., Welsh, D. T., Teasdale, P. R., Grice, K., Vacher, M., Bennett, W. W. & Visscher, P. T. 2014 Diel fluctuations in solute distributions and biogeochemical cycling in a hypersaline microbial mat from Shark Bay, WA. *Marine Chemistry* **167**, 102–112.

Pfeffer, C., Larsen, S., Song, J., Dong, M., Besenbacher, F., Meyer, R. L., Kjeldsen, K. U., Schreiber, L., Gorby, Y. A., El-Naggar, M. Y., Leung, K. M., Schramm, A., Risgaard-Petersen, N. & Nielsen, L. P. 2012 Filamentous bacteria transport electrons over centimetre distances. *Nature* **491** (7423), 218–221.

Rabouille, C., Caprais, J. C., Lansard, B., Crassous, P., Dedieu, K., Reyss, J. L. & Khripounoff, A. 2009 Organic matter budget in the Southeast Atlantic continental margin close to the Congo Canyon: in situ measurements of sediment oxygen consumption. *Deep-Sea Research Part II: Topical Studies in Oceanography* **56** (23), 2223–2238.

Revsbech, N. P., Jørgensen, B. B. & Blackburn, T. H. 1980 Oxygen in the sea bottom measured with a microelectrode. *Science* **207** (4437), 1355–1356.

Sato, C., Nakayama, K. & Furukawa, K. 2012 Contributions of wind and river effects on DO concentration in Tokyo Bay. *Estuarine, Coastal and Shelf Science* **109**, 91–97.

Schwermer, C. U., Ferdelman, T. G., Stief, P., Gieseke, A., Rezakhani, N., Van Rijn, J., De Beer, D. & Schramm, A. 2010 Effect of nitrate on sulfur transformations in sulfidogenic sludge of a marine aquaculture biofilter. *FEMS Microbiology Ecology* **72** (3), 476–484.

Sugahara, S., Yurimoto, T., Ayukawa, K., Kimoto, K., Senga, Y., Okumura, M. & Seike, Y. 2010 A simple in situ extraction method for dissolved sulfide in sandy mud sediments followed by spectrophotometric determination and its application to the bottom sediment at the northeast of Ariake Bay. *BUNSEKI KAGAKU* **59** (12), 1155–1161.

Valdemarsen, T., Kristensen, E. & Holmer, M. 2009 Metabolic threshold and sulfide-buffering in diffusion controlled marine sediments impacted by continuous organic enrichment. *Biogeochemistry* **95** (2), 335–353.

Zhu, Q. & Aller, R. C. 2010 A rapid response, planar fluorosensor for measuring two-dimensional pCO_2 distributions and dynamics in marine sediments. *Limnology and Oceanography: Methods* **8**, 326–336.

First received 3 May 2016; accepted in revised form 26 October 2016. Available online 23 November 2016